Computers and Concrete, *Vol. 22, No. 1 (2018) 39-51*
DOI: https://doi.org/10.12989/cac.2018.22.1.039

An efficient algorithm for scaling problem of notched beam specimens with various notch to depth ratios

Mohammad Karamloo[a] and Moosa Mazloom[*]

Department of Civil Engineering, Shahid Rajaee Teacher Training University, Lavizan, Tehran, Iran

(Received December 12, 2017, Revised March 19, 2018, Accepted April 13, 2018)

Abstract. This study introduces a new algorithm to determine size independent values of fracture energy, fracture toughness, and fracture process zone length in three-point bending specimens with shallow to deep notches. By using the exact beam theory, a concept of equivalent notch length is introduced for specimens with no notches in order to predict the peak loads with acceptable precisions. Moreover, the method considers the variations of fracture process zone length and effects of higher order terms of stress field in each specimen size. In this paper, it was demonstrated that the use of some recently developed size effect laws raises some concerns due to the use of nonlinear regression analysis. By using a comprehensive fracture test data, provided by Hoover and Bazant, the algorithm has been assessed. It could be concluded that the proposed algorithm can facilitate a powerful tool for size effect study of three-point bending specimens with different notch lengths.

Keywords: concrete; fracture mechanics; civil engineering structures; fracture toughness; notch length

1. Introduction

Since 1969, when Leicester published his pioneering research (Leicester 1969), the study of size effect phenomenon has gathered lots of attention within researchers. Recently, this field of interest not only was of the most important subjects in fracture mechanics but also it extended to be used in different aspects of engineering problems, material testing, and numerical solutions. For instance, Yoo and Yang studied the effect of beam size on shear behavior of high strength concrete beams (Yoo and Yang 2018). Their test results showed that the increase of beam size decreases the shear strength of the beams significantly. They further reported that this effect was more prevalent for beams cast of fiber-reinforced high-performance concrete than for those without fibers. The age-dependent size effect and fracture characteristics of ultra-high performance concrete were investigated by (Wan-Wendner *et al*. 2018). They performed both aging and size effect tests on notched three point bending specimens as well as using simulation methods. Rong and his co-workers considered the effects of specimen size and thermal-damage on physical and mechanical behavior of a fine-grained marble (Rong *et al*. 2018). Their uniaxial compression tests have been carried out on specimens of diameters 2, 50, 75, and 100 mm under different treatment temperatures. They reported that both the specimen size and thermal damage have significant influence on the rock strength and deformation behavior. Needleman investigated the effect of size on necking of dynamically loaded notched bars and reported that the location of necking depends on the size of the specimen (Needleman 2018). The statistical size effect was studied on flexural strength of steel members (Li and Pasternak 2018). The size effect was included in discrete element modeling of quasi-brittle solids by (Liu *et al*. 2018). They used an exponential softening contact bonds model, which is tied to input fracture energy and addresses particle size issue to model the size effect. In another statistical vision for study of size effect, Lei proposed a generalized weakest-link model for size effect on strength of quasi-brittle materials (Lei 2018). The influences of size and shape of specimen on compressive strength of concrete have been assessed and the results of dynamic and static tests showed major dependency between the results and the size and shape of specimens (Li *et al*. 2018).

Generally, quasi-brittle fracture behavior is a failure process in which a large fracture process zone along with a small hardening plasticity zone takes place prior to peak load (Malíková and Veselý 2015). In this kind of materials, such as concrete, the multi-parameter fracture mechanics approach is necessary since the stress field is to be investigated at larger distances from the crack tip (Malíková and Veselý 2015). Besides, as reported by (Malíková and Veselý 2015), the lower stress levels or stress fields farther from the crack tip should be constructed by higher order terms. However, indicating the sufficient number of higher order terms is too case dependent (Malíková and Veselý 2015). The influence of higher order terms on crack-tip stress field is of great importance. In this regard, some important studies have been reported in the literature about the higher order terms and three-dimensional effects. Berto and Lazzarin investigated the influence of higher order terms on the stress field of a cracked plate under plane loading (Berto and Lazzarin 2010). They also presented a

*Corresponding author, Associate Professor
E-mail: moospoon@yahoo.com; mazloom@sru.ac.ir
[a]Ph.D.
E-mail: m.karamloo@sru.ac.ir

ISSN: 1598-8198 (Print), 1598-818X (Online)

set of equations for accurately describing the stress field ahead of the crack tip, particularly for cases with mix mode condition (Berto and Lazzarin 2013). Berto and his co-workers in a valuable study reviewed the application of strain energy density for brittle and quasi-brittle failure assessment of graphite, which is a quasi-brittle solid (Berto *et al*. 2013). Anti-plane shear loading on sharp notches or cracks could lead to a generation of coupled in plane singular shear stress field, while this mode was widely ignored in the stress analysis of notched components (Berto *et al*. 2013). Berto and his co-workers investigated the mentioned mode by means of 3D finite element method, which was applied to notched plated with different notch opening angles and plate thicknesses (Berto *et al*. 2013). According to their study, the stress field corresponding to the coupled mode is localized and quickly diminishes with the distance from the crack tip. Zappalorto and Lazzarin studied the features of three-dimensional elastic stress field ahead of the notches in finite thick plates under different loading regimes (Zappalorto and Lazzarin 2013). It is worth noting that the influence of higher order terms tied to mode II loading on the out of plane singular mode has been investigated by Berto *et al*. (2011). A valuable retrospective review of three-dimensional effects at cracks and sharp notches was published by Pook (2013). However, the review was limited to linear elastic, homogenous, isotropic materials, with yielding confined to a small region at the crack tip. Kotousov and his co-workers investigated the effect of thickness on elastic deformation and quasi-brittle fracture of plate components (Kotousov *et al*. 2010).

Apart from all researches regarding size effect phenomenon in quasi brittle material, and particularly concrete (Xiao and Karihaloo 2006, Karihaloo and Xiao 2007, Xiao and Karihaloo 2007, Karihaloo and Xiao 2008, Karihaloo and Xiao 2010, Muralidhara *et al*. 2011, Cifuentes and Karihaloo 2013, Karihaloo *et al*. 2013, Ramachandra Murthy *et al*. 2013, Ramachandra Murthy *et al*. 2013, Hoover and Bažant 2014, Hoover and Bažant 2014, Hoover and Bažant 2014, Alyhya *et al*. 2016, Karamloo *et al*. 2016, Karamloo *et al*. 2016, Karamloo *et al*. 2017, Mazloom *et al*. 2017, Lei 2018), there are still debates on theoretical ground of this phenomenon. Bazant and his co-workers were confidently of the most inspiring scientists in this field after 1980's. They published many papers and clarified many ambiguous points in the field. The study of deterministic size effect in quasi-brittle materials such as concrete, rock, sea ice, etc. goes back to 1976, when Hillerborg *et al*. (1976) pioneered a cohesive crack model (fictitious crack model) by means of finite element analysis and modifying the Dugdale model for crack-tip plasticity to include the effects of quasi-brittle behavior of concrete. Then, Bazant and Oh (1983) proposed the crack band theory for heterogeneous aggregate material, which exhibits gradual softening due to micro-cracking, in mode I loading. They modeled the fracture as a blunted smeared crack band to derive a simple tri-axial stress-strain relation, which was able to describe the effects of gradual micro cracking. Bazant attributed the size effect to the blunted region ahead of the crack-tip and assumed that the width of this zone is constant and relative to maximum nominal size of aggregate (Bazant 1984). The analysis of this model rests on the hypothesis that the released energy caused by fracture, depends on both the area and the length of crack band (Bazant 1984). The model then exploited by Bazant *et al*. for determination of the parameters of R-curve, crack band model, and fictitious crack model without measuring crack length or unloading compliance (Bazant *et al*. 1986). Bazant and Pfeiffer (1987) and Bazant and Kazemi (1990) investigate the effects of specimen shape and size on fracture energy of material, which must be constant in all shapes and sizes based on its definition. These studies showed that the proposed law of Bazant *et al*. could describe the effects of size and shape of the specimen on fracture parameters and load carrying capacity of the specimens with relatively large cracks. Further researches showed that the length of notch (pre-crack) could have prevalent effects on the results of the mentioned model. This concern was one of the most challenging issues in the fracture mechanics of quasi-brittle solids. Duan *et al*. (2003) were of researchers who tried to explain the effects of relative crack length of specimens on fracture parameters. They used the concepts of "local fracture energy distribution" and "boundary effects" to explain the size effects on fracture parameters of concrete. Duan *et al*. (Duan *et al*. 2006, Duan *et al*. 2007), Hu and Duan (2004, 2007, 2009), pioneered their analysis on the basis of two hypothesis: 1) The size-dependent quasi-brittle fracture transition is due to the interactions of the nearest boundary with the FPZ, instead of size variations. 2) The widely accepted Bazant's size effect law, which holds in geometrically similar specimens, is a special case of Hu-Duan's model. These hypotheses were criticized on theoretical ground by Yu *et al*. (2010). They illustrated an example in which the boundary was too far but the strongest size effect (i.e., LEFM) existed. In addition, two instances were illustrated in which the FPZ could increase or decrease the size effect. The cohesive stress analyses, which were reported by Cedolin and Cusatis (2008), Cusatis and Schauffert (2009), were in line with this assertion. Therefore, one can conclude that the former hypothesis was erroneous. Furthermore, the assumed stress profile at varying crack length, and the matched asymptote for large-size structures with no notch, were of the most important problematic aspects, which were criticized by Yu *et al*. (2010).

Generally, six asymptotic cases can be distinguished for cohesive fracture of quasi-brittle materials: 1) the behavior of very small structures; 2) the behavior of very large structures; 3) structures with no notch; 4) structures with deep notches; 5) structures in which purely statistical Weibull-type (Weibull 1939, Weibull 1951) size effect governs; 6) structures with purely deterministic size effect. The aim to build a bridge between these six cases was a motivation for Bazant and Yu to propose a universal size effect law by which these asymptotic cases could be connected smoothly (Bazant and Yu 2009). However, further experiments by Hoover *et al*. (Hoover *et al*. 2013) showed that the Type I-Type II transition in this law (study of Yu and Bazant) yields erroneous results (Hoover and Bažant 2014). Hence, a new size effect law, called

"universal size-shape effect law", were proposed by Hoover and Bazant (2014). Although Hoover and Bazant stated that this model could handle all the asymptotic cases, it is shown in the present study that the use of statistical methods of nonlinear curve fitting could result in different values of fracture parameters. Consequently, the precisions of predictions could be affected by these differences. In other words, the universal size effect law of Bazant and his co-workers is an eighteen-parameter equation, which needs nonlinear techniques for curve fitting to be used (Hu *et al*. 2017).

Recently, researchers conducted experimental and analytical studies about the effects of higher order terms of stress field. For example, the influence of higher order terms of Williams's series on accuracy of the description of stress fields around the tip of the crack were investigated by some researchers (Malíková and Veselý 2015). Malíková and Veselý also discussed the significance of the multi-parameter fracture mechanics approach especially in failure of quasi-brittle materials and estimation of plastic zone extent. By using the meso-scale modeling approach, Aissaoui and Matallah (2017) analytically investigated the classical Bazant SEL and a new size effect law based on enrichment of the stress field of the crack tip. Berto *et al*. (2011) investigated the effects of higher order terms , tied to mode II loading, on out of plane singular mode. Akbardoost and Rastin (2015) investigated the effects of higher order terms of crack-tip stress field for two disk-type specimens under wide range combination of mixed-mode I/II loading.

The aim of this study is to review the universal size-shape effect law (USSEL) and propose a new stress based law, which is able to predict deterministic size effects in three point bending specimens with shallow to deep notches. To do so, a summary review of USSEL is presented in the following section.

2. Brief review of USSEL and problem statement

For a crack, which is neither large nor negligible, at failure, a smooth transition between Type 2 and Type 1 size effect was proposed by Hoover and Bazant (2014) as follows

$$\sigma_N = \left[\frac{E'G_f}{g_0 D + (1-\lambda)c_f g_0' + \lambda E' G_f / f_{r\infty}^2}\right]^{-0.5} \left(1+\frac{r\lambda D_b}{\bar{D}+l_p}\right)^{1/r} \quad (1)$$

in which

$$\lambda = e^{-\left(\frac{\alpha_0^k (\bar{D}/d_a)^p}{q}\right)} \quad (2)$$

is a Type 1 to Type 2 transition parameter, where α_0 is initial span/depth ratio, and d_a is maximum nominal size of the aggregate. G_f, c_f, $f_{r\infty}$, D_b, r, k, p, q, and l_p, are parameters to be calibrated by data fitting, g_0 is non-dimensional energy release rate function, and g_0' is derivative of g_0 with respect to α_0 (notch/depth ratio). Hoover and Bazant defined $\bar{D}$ as

$$\bar{D} = \frac{2\varepsilon}{\psi \varepsilon_{,n}} \quad (3)$$

where $\varepsilon_{,n}$ is strain gradient and equals to $\partial\varepsilon/\partial x_n$, factor $\psi\left(Span/Depth\right)$ is shape factor, which was defined as 1 for slender beams. Based on elastic stress analysis, they defined the shape factor for span/depth ratio of tested beams (2.176), as 0.896. They derived Eq. (1) such that it yields Type 1 size effect for α=0, and Type 2 size effect for deep notches. There are a few points, which are questionable.

1. For the tested beams, which were not slender, a shape factor was defined. As stated previously, they used exact elastic solution of elasticity theory of beams and derived

$$\frac{\varepsilon}{\varepsilon_{,n}} = \frac{\psi}{2} D \quad (4)$$

If someone merge Eqs. (4) and (3), it would yield

$$D = \bar{D} \quad (5)$$

Therefore, the question is why this factor is defined.

2. The other point is about the optimization algorithms, which are needed for nonlinear curve fitting e.g., trust-region-reflective optimization algorithm (Coleman and Li 1992, Coleman and Li 1996), or Levenberg-Marquardt algorithm (Moré 1978). It will be shown in the subsequent sections that these methods could yield far different parameters according to the bounds or start point selection. Therefore, an efficient method is proposed for capturing the size effect of concrete structures and consequently, to determine the fracture parameters by linear regression, which could yield more reliable results.

According to the mentioned issues regarding the use of USSEL as well as computational burden of estimating of needed parameters in Eq. (1) and Eq. (2), the use of USSEL is somehow cumbersome. In this paper, an efficient algorithm has been presented in which the effects of higher order terms of stress field have been considered as well as the effect of the size of FPZ on fracture parameters. In fact, in contrast to Bazant's SEL, the proposed algorithm calculates the size of FPZ based on Williams' solution along with maximum tangential stress criterion. Accordingly, this algorithm could circumvent the mentioned concern raised by Hu, Duan, and their co-workers. It is worth noting that Hu and his co-workers recently modified their methods to include the influence of maximum size of aggregate in concrete (Hu *et al*. 2017). However, to the authors' knowledge, the effects of this parameter were considered in the earlier studies of Bazant and his co-workers. Of course, the mentioned contribution of professor Hu is so valuable in many aspects and can shed light on our understanding about the fracture behavior of concrete. Thanks to the use of higher order terms of Williams's expansion, the method could be extended to include the effect of T-stresses as well as mixed mode condition. However, the inclusion of these parameters was beyond the scope of this study. The other main contribution about the effects of size on fracture parameters of concrete is the study of Ayatollahi and Akbardoost (2012). In the mentioned study, by using the

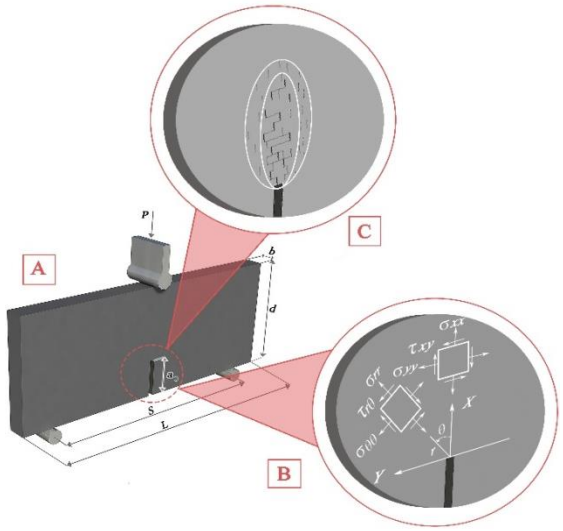

Fig. 1 (a) Three-point bending configuration. (b) Crack-tip coordinate system. (c) Fracture process zone

first three terms of Williams's expansion, the effect of size on fracture toughness of concrete has been assessed. However, the variation of notch length and the cases with the so-called Type I size effect was not considered. In the present study, the exact beam theory has been used to introduce the concept of equivalent notch length for beams with no notch. Besides, the first five terms of Williams's expansion have been used which could lead to better precisions of the peak loads.

3. Proposed size-FPZ dependent criterion

According to the published literature (Hillerborg *et al*. 1976, Bazant and Oh 1983, Bazant 1984), propagation of a crack in a quasi-brittle solid is preceded by localization of micro-cracks in a limited zone ahead of a crack-tip, called fracture process zone (FPZ). These micro-cracks become inter-connected as the load increases and consequently, the fracture would take place (see Fig. 1(c)). Since the material exhibits softening behavior in FPZ, the LEFM, explicitly, does not hold in quasi-brittle materials such as concrete. Therefore, the effective elastic crack model and cohesive crack model have been proposed in the literature. As stated in the previous sections, one of the most famous theories, describing the behavior of the crack-tip in concrete, is fictitious crack model by Hillerborg (Hillerborg *et al*. 1976). Based on this model, a crack will initiate in concrete if a normal-to-crack component of the stress field reaches tensile strength of concrete f_t. Williams's series expansion is one of the most well-known solutions, describing the stress and displacement fields near the crack-tip (Williams 1961). According to Williams's expansion, one can determine the normal-to-crack component of stress field as

$$\sigma_{yy}=\sum_{n=1}^{\infty}\frac{n}{2}r^{\frac{n}{2}-1}a_n\begin{bmatrix}\left(2-\frac{n}{2}-(-1)^n\right)\cos\left(\frac{n}{2}-1\right)\theta+\ldots\\ \ldots+\left(\frac{n}{2}-1\right)\cos\left(\frac{n}{2}-3\right)\theta\end{bmatrix} \quad (6)$$

where r and θ are polar coordinates, illustrated in Fig. 1(b), n is the order of terms in series expansion, and a_n are coefficients, which reflect the effects of geometry and loading mode.

In this study, only mode I condition is going to be considered. Hence, by setting θ=0, and considering the first five terms of Williams's expansion, one can write

$$\sigma_{yy}=a_1/\sqrt{r}+3a_3r^{0.5}+5a_5r^{1.5} \quad (7)$$

Based on Hillerborg's assumption, the crack initiates when $\sigma_{\theta=0}$ reaches f_t. Moreover, as stated in the previous sections, the importance of including the higher order terms of stress field around the crack-tip is obvious (Karihaloo and Xiao 2001, Ayatollahi and Nejati 2011, Ayatollahi and Akbardoost 2012, Ayatollahi and Akbardoost 2013, Ayatollahi and Akbardoost 2013, Khoramishad *et al*. 2013). Hence, by using the idea of including higher order terms of stress field in size effect study (Ayatollahi and Akbardoost 2012, Ayatollahi and Akbardoost 2013, Ayatollahi and Akbardoost 2013, Khoramishad *et al*. 2013) along with the assumptions of effective elastic crack model, it could be written that

$$a_1/\sqrt{r}+3a_3r^{0.5}+5a_5r^{1.5}=f_t \quad (8)$$

In order to solve the Eq. (8), the coefficients should be normalized as

$$a_1^*=\frac{a_1}{\sigma_N d^{0.5}} \quad (9)$$

$$a_3^*=a_3d^{0.5}/\sigma_N \quad (10)$$

$$a_5^*=d^{1.5}\left(a_5/\sigma_N\right) \quad (11)$$

Substituting Eqs. (9)-(11) to Eq. (8), one can obtain

$$\sigma_N=\frac{f_t}{a_1^*\left(\frac{d}{r}\right)^{0.5}+3a_3^*\left(\frac{r}{d}\right)^{0.5}+5a_5^*\left(\frac{r}{d}\right)^{1.5}} \quad (12)$$

As stated in the preceding sections, Hu and Duan (2004), Duan *et al*. (2003, 2003, Duan *et al*. 2006, 2007), claimed that the interactions between FPZ and the neighboring boundaries governs the size effects rather than the size of specimen. In contrast, the studies of Yu *et al*. (2010), Hoover and Bazant (2014) showed that the FPZ could have effect on size effects, nevertheless these effects could not lead to a conclusion that the size of specimen is not important. Eq. (12) is a stress-based size effect criterion, which includes the effects of FPZ dimension as well as the effects of specimen size, on the size effect criterion. Moreover, it can include the effects of higher order terms of stress field, whose effects are significant in fracture behavior of structures (Karihaloo and Xiao 2001, Karihaloo and Xiao 2001, Berto *et al*. 2011).

The other advantage of this criterion is that it could be manipulated for determination of apparent fracture

toughness (K_C). To do so, it is assumed that the a_1, reflects only the effects of mode I stress intensity factor as (Owen and Fawkes 1983, Karihaloo and Xiao 2001)

$$a_1 = K_I \Big/ \sqrt{2\pi} \tag{13}$$

Thus, one can obtain the apparent toughness criterion as

$$K_C = \frac{f_t\sqrt{2\pi d}}{\left(\frac{d}{r}\right)^{0.5} + 3\left(\frac{a_3^*}{a_1^*}\right)\left(\frac{r}{d}\right)^{0.5} + 5\left(\frac{a_5^*}{a_1^*}\right)\left(\frac{r}{d}\right)^{1.5}} \tag{14}$$

The normalized higher order coefficients are obtainable using hybrid-crack-element method, originally proposed by Tong *et al*. (1973), and extended by Karihaloo and Xiao (2001, 2001), as

$$a_1^* = \frac{\sqrt{\alpha}}{\sqrt{2\pi}(1-\alpha)^{1.5}(1+3\alpha)}\left\{\begin{matrix} F_\infty(\alpha)+... \\ ...+\frac{4}{\beta}\left[F_4(\alpha)-F_\infty(\alpha)\right] \end{matrix}\right\} \tag{15}$$

$$a_3^* = t_\infty(\alpha) + \frac{4}{\beta}\left[t_4(\alpha) - t_\infty(\alpha)\right] \tag{16}$$

$$a_5^* = h_\infty(\alpha) + \frac{4}{\beta}\left[h_4(\alpha) - h_\infty(\alpha)\right] \tag{17}$$

where $F_4(\alpha)$, $F_\infty(\alpha)$, $t_\infty(\alpha)$, $t_4(\alpha)$, $h_\infty(\alpha)$, and $h_4(\alpha)$, are auxiliary functions, which can be found for three point bending configuration in Karihaloo and Xiao's study (Karihaloo and Xiao 2001), and β is span/depth ratio of specimen.

4. Determination of size dependent length of FPZ

In order to use Eq. (12) and Eq. (14), the values of size dependent length of fracture process zone should be calculated. To do so, the recorded values of nominal strength should set to be equal to Eq. (12). Hence, Eq. (18) should be solved for each specimen.

$$A^*X^4 + B^*X^3 + C^*X^2 + D^*X + E^* = 0 \tag{18}$$

in which $A^* = 25\left(\frac{\sigma_N}{f_t}\right)\left(a_5^*\right)^2$, $B^* = 30\left(\frac{\sigma_N}{f_t}\right)\left(a_5^*\right)\left(a_3^*\right)$, $C^* = \left(\frac{\sigma_N}{f_t}\right)\left(10a_1^*a_5^* + 9\left(a_3^*\right)^2\right)$, $D^* = 6\left(\frac{\sigma_N}{f_t}\right)\left(a_1^*\right)\left(a_3^*\right) - 1$, and $E^* = \left(\frac{\sigma_N}{f_t}\right)\left(a_1^*\right)^2$. Then one can obtain r as

$$r = X.d \tag{19}$$

It should be noted that the minimum real positive root of Eq. (18) should be substituted in Eq. (19) for determination of r. The other important ambiguity that should be clarified is the asymptotic values of r. In other words, the changes of FPZ length should be nearly constant in large specimens. The studies of Karihaloo (1999), Bazant *et al*. (1991) are of the most significant instances for description of the relation between r, specimen depth, and the asymptotic value of FPZ length (r_∞). Bazant *et al*. considered geometric nonlinearity in propagation of a crack and described the size dependency of FPZ based on fracture energy approach as (Bazant *et al*. 1991)

$$r_\infty = r\frac{g(\alpha_0)}{g'(\alpha_0)} \Big/ \left(\frac{g(\alpha)}{g'(\alpha)} - \frac{r}{d}\right) \tag{20}$$

where $\alpha=\alpha_0+r/d$, $g(\alpha)$ is non-dimensional fracture energy, and $g'(\alpha)$ is derivative of $g(\alpha)$ to α. Bazant *et al*. proposed Eq. (20) for determination of size and geometry dependent R-curves (Bazant *et al*. 1991), however it did not affect the size effect plot in the Bazant's method. Is Eq. (20) suitable for the proposed method of this paper? Actually, no! To consider the suitability of this equation, Eq. (20) is mathematically manipulated and the Taylor's series expansion of the method is calculated as

$$r = \frac{C_b}{C_b - d}\left(\begin{matrix} -193.12\alpha^5 + ... \\ ...+459.033\alpha^4 + 15.384\alpha^3 - ... \\ ...-2.568\alpha^2 - \alpha \end{matrix}\right) \tag{21}$$

where C_b is a constant, which could be determined in terms of $g(\alpha_0)$, $g'(\alpha_0)$, and r_∞. As can be seen, when the size of specimen approaches infinity, $r\to 0$; when the size of specimen approaches to zero, the r approaches a constant value. Instead, it is well-known that the size of fracture process zone should approach a constant value (i.e., r_∞) for large specimens. Therefore, this function is not suitable to be used in the proposed method. There are two critical condition for variation of r versus d: 1) the length of FPZ approaches constant value for large specimens, 2) for small specimens, the FPZ length is small. Are these conditions sufficient for defining a suitable function? Not really. According to these conditions, one can use a simple function as

$$r = A e^{\frac{-B}{d}} \tag{22}$$

where A and B are empirical constants, which can be obtained by regression analysis. Considering Eq. (22), it is apparent that this relation satisfies both conditions. Whereas, it is not suitable to be used. The substitution of Eq. (22) into Eq. (12) yields

$$\left(\frac{\sigma_N}{f_t}\right) = \left(\frac{1}{a_1^*}\right)\frac{\left(\frac{A e^{\frac{-B}{2d}}}{\sqrt{d}}\right)}{1 + 3\frac{a_3^*}{a_1^*}\left(\frac{A e^{\frac{-B}{d}}}{d}\right) + 5\frac{a_5^*}{a_1^*}\left(\frac{A e^{\frac{-B}{d}}}{d}\right)^2} \tag{23}$$

Considering Eq. (23), one can conclude that when $d\to\infty$, LEFM does not govern (size effect plot does not approach, in the doubly logarithmic plot, an asymptote of slope -1/2). Moreover, Eq. (23) does not approach strength criterion for small specimens. These observations are not in line with reality. Hence, Eq. (22) is not a suitable function.

Karihaloo (1999), assumed that the crack-tip opening displacement ($CTOD_C$) is a constant material property and used the Hillerborg's model for FPZ. Afterwards, he

Table 1(a) Dimensions of specimens and their corrected peak loads (a/d=0.3)

Series	Depth, d (mm)	Span, S (mm)	Thickness, b (mm)	a/d	Corrected peak loads P^0 (kN)
AL0.3	500	1088	40	0.3	11.581
	500	1088	40	0.3	11.336
	500	1088	40	0.3	12.316
	500	1088	40	0.3	10.907
	500	1088	40	0.3	11.029
	500	1088	40	0.3	12.132
	215	468	40	0.3	6.271
	215	468	40	0.3	7.061
	215	468	40	0.3	6.877
	215	468	40	0.3	7.509
	215	468	40	0.3	6.297
	215	468	40	0.3	6.323
	93	202	40	0.3	3.203
	93	202	40	0.3	3.567
	93	202	40	0.3	3.385
	93	202	40	0.3	3.590
	93	202	40	0.3	3.453
	93	202	40	0.3	3.453
	93	202	40	0.3	3.533
	93	202	40	0.3	3.533
	40	87	40	0.3	1.819
	40	87	40	0.3	1.525
	40	87	40	0.3	1.578
	40	87	40	0.3	1.662
	40	87	40	0.3	2.260
	40	87	40	0.3	1.941
	40	87	40	0.3	2.010
	40	87	40	0.3	1.642

Table 1(b) Dimensions of specimens and their corrected peak loads (a/d=0.15)

Series	Depth, d (mm)	Span, S (mm)	Thickness, b (mm)	a/d	Corrected peak loads P^0 (kN)
AL0.15	500	1088	40	0.15	18.260
	500	1088	40	0.15	18.321
	500	1088	40	0.15	17.402
	500	1088	40	0.15	17.402
	500	1088	40	0.15	18.627
	500	1088	40	0.15	17.524
	215	468	40	0.15	9.406
	215	468	40	0.15	9.722
	215	468	40	0.15	9.801
	215	468	40	0.15	10.302
	215	468	40	0.15	9.169
	215	468	40	0.15	9.722
	93	202	40	0.15	5.858
	93	202	40	0.15	5.391
	93	202	40	0.15	5.243
	93	202	40	0.15	5.322
	93	202	40	0.15	4.992
	93	202	40	0.15	4.787
	93	202	40	0.15	4.912
	93	202	40	0.15	4.889
	40	87	40	0.15	2.422
	40	87	40	0.15	2.819
	40	87	40	0.15	2.417
	40	87	40	0.15	2.662
	40	87	40	0.15	2.569
	40	87	40	0.15	2.627
	40	87	40	0.15	2.853
	40	87	40	0.15	2.593
	40	87	40	0.15	2.490
	40	87	40	0.15	2.936

reported that the size dependent length of fracture process zone is related to its asymptotic value and size of specimen as

$$r_\infty = r\left(1-0.5\left(\frac{r_\infty}{d}\right)\left(\frac{g'(\alpha_0)}{g(\alpha_0)}\right)\right) \tag{24}$$

By using the mathematical manipulation, one can write Eq. (24) as

$$r = \frac{A_0 d}{d + B_0} \tag{25}$$

in which A_0=r_∞, and $B_0 = -0.5\frac{g'(\alpha_0)}{g(\alpha_0)}r_\infty$ are empirical coefficient, which are also obtainable from linear regression analysis. Substituting Eq. (25) into Eq. (12), one can obtain a size effect law as

$$\sigma_N = \frac{f_t\sqrt{A_0}}{a_1^*\sqrt{(B_0+d)}} \times \frac{1}{1+3\frac{a_3^*}{a_1^*}\left(\frac{A_0}{B_0+d}\right)+5\frac{a_5^*}{a_1^*}\left(\frac{A_0}{B_0+d}\right)^2} \tag{26}$$

It is apparent that both Eqs. (25) and (26) satisfies the mentioned conditions and this function could be a suitable selection for the proposed method. Eq. (25) is similar to equation, which was proposed by Ayatollahi and Akbardoost (2012).

5. Experimental data

Progress in the modeling of concrete fracture and introduction of these concepts to practitioners and scientists has major dependency on availability of comprehensive database for fracture. There are a vast number of fracture data in the literature (Bazant and Pfeiffer 1987, Bazant and Planas 1998, Bazant and Becq-Giraudon 2002, Karihaloo, Abdalla *et al*. 2003), nevertheless they cover limited range of α_0, and specimen size. In addition, the tests have been performed on different batches of concrete at different ages and different conditions with various test procedures. Combination of all these data produces a database, which is prone to a scatter of data that makes modelling very difficult. Fortunately, Hoover and his co-workers remedied this situation by performing comprehensive fracture tests on the specimens made from same batch of one typical

Table 1(c) Dimensions of specimens and their corrected peak loads (a/d=0.075)

Series	Depth, d (mm)	Span, S (mm)	Thickness, b (mm)	a/d	Corrected peak loads P^0 (kN)
AL0.075	500	1088	40	0.075	24.203
	500	1088	40	0.075	21.385
	500	1088	40	0.075	23.897
	500	1088	40	0.075	24.265
	500	1088	40	0.075	21.017
	500	1088	40	0.075	18.750
	215	468	40	0.075	12.225
	215	468	40	0.075	11.435
	215	468	40	0.075	11.988
	215	468	40	0.075	13.148
	215	468	40	0.075	11.883
	215	468	40	0.075	11.909
	93	202	40	0.075	6.359
	93	202	40	0.075	6.291
	93	202	40	0.075	6.371
	93	202	40	0.075	6.508
	93	202	40	0.075	6.804
	93	202	40	0.075	7.499
	93	202	40	0.075	6.804
	93	202	40	0.075	7.853
	40	87	40	0.075	2.946
	40	87	40	0.075	3.304
	40	87	40	0.075	3.274
	40	87	40	0.075	3.167
	40	87	40	0.075	3.260
	40	87	40	0.075	3.451
	40	87	40	0.075	3.721
	40	87	40	0.075	3.304
	40	87	40	0.075	3.118

Table 1(d) Dimensions of specimens and their corrected peak loads (a/d=0.025)

Series	Depth, d (mm)	Span, S (mm)	Thickness, b (mm)	a/d	Corrected peak loads P^0 (kN)
AL0.025	500	1088	40	0.025	32.475
	500	1088	40	0.025	26.409
	500	1088	40	0.025	30.637
	500	1088	40	0.025	30.392
	500	1088	40	0.025	24.632
	500	1088	40	0.025	28.615
	215	468	40	0.025	14.149
	215	468	40	0.025	13.754
	215	468	40	0.025	14.254
	215	468	40	0.025	14.992
	215	468	40	0.025	14.202
	215	468	40	0.025	12.805

concrete of same age and curing conditions (Hoover *et al*. 2013). Their tests were carried out on three-point bending specimens of size range 1:12.5 and notch/depth ratios from zero to 0.3. Table 1 (a)-(e) shows the values of corrected peak loads (according to weight of each specimen) for each specimen according to Hoover *et al*. (2013). It should be noted that the tensile strength of the concrete was 6.72 MPa and the modulus of elasticity was reported 41.24 GPa.

Table 1(e) Dimensions of specimens and their corrected peak loads (a/d=0.0)

Series	Depth, d (mm)	Span, S (mm)	Thickness, b (mm)	a/d	Corrected peak loads P^0 (kN)
AL0.0	500	1088	40	0	30.147
	500	1088	40	0	34.498
	500	1088	40	0	35.723
	500	1088	40	0	34.620
	500	1088	40	0	34.804
	500	1088	40	0	38.971
	215	468	40	0	16.362
	215	468	40	0	22.290
	215	468	40	0	16.415
	215	468	40	0	21.816
	215	468	40	0	17.785
	215	468	40	0	15.782
	93	202	40	0	8.400
	93	202	40	0	7.921
	93	202	40	0	8.434
	93	202	40	0	8.001
	93	202	40	0	8.764
	93	202	40	0	7.682
	40	87	40	0	3.735
	40	87	40	0	3.706
	40	87	40	0	3.588
	40	87	40	0	3.613
	40	87	40	0	4.255
	40	87	40	0	4.201
	40	87	40	0	3.515

5. Results and discussion

In the previous sections, a new size effect law has been proposed for size effect studies. In this section, two sub-sections are presented in which the USSEL is discussed and the results of the proposed algorithm are compared with the Bazant's method. To do so, the nominal stress σ_N should be determined for each specimen as

$$\sigma_N = \frac{3P^0 S}{2bd^2} \tag{27}$$

Afterwards, the values of a_1^*, a_3^*, and a_5^* should be obtained by using Eqs. (9)-(11). One can find the empirical coefficients of A_0, and B_0 by plotting the data of $x=d^{-1}$, and $y=r^{-1}$ for each group and fitting a regression line as

$$y = px + q \tag{28}$$

where $p = \frac{B_0}{A_0}$, and $q = \frac{1}{A_0}$.

5.1 Ambiguity of using USSEL

As stated briefly in section 2, for determination of fracture parameters by USSEL, there is a need to use

Table 2 Effects of selecting the start point and bounds on trust-region-reflective method

		Try 1	Try 2	Try 3	Try 4	Try 5
Bounds	D_b	$(-\infty,+\infty)$	$(-\infty,+\infty)$	$(-\infty,+\infty)$	(0,100)	(0,500)
	l_p	$(-\infty,+\infty)$	$(-\infty,+\infty)$	$(-\infty,+\infty)$	(0,500)	(0,500)
	$f_{r\infty}$	$(-\infty,+\infty)$	$(-\infty,+\infty)$	(0,+∞)	(0,10)	(0,10)
	r	$(-\infty,+\infty)$	$(-\infty,+\infty)$	(0.49,2)	(0.49,2)	(0.49,2)
Start points	D_b	0.9549	80	80	80	80
	l_p	0.9134	130	130	130	130
	$f_{r\infty}$	0.2722	5	5	5	5
	r	0.0843	0.5	0.5	0.5	0.5
R-square	R^2	_	0.5239	0.5665	0.5301	0.5614
Fitted equation	D_b	The optimization did not converge	243.4	985.1	99.96	465.6
	l_p		19.72	601.5	182.2	491.4
	$f_{r\infty}$		4.826	3.11	5.194	3.865
	r		6.876	1.073	0.4915	0.6419

nonlinear regression analysis and consequently, using optimization methods such as trust-region-reflective or Levenberg-Marquardt algorithms. For instance, let us check the trust-region-reflective method for specimens with α=0. Hoover and Bazant (2014) carried out a nonlinear regression analysis for fitting Eq. (1) by using trust-region-reflective optimization algorithm and reported the parameters as

$$D_b = 73.2 \text{ mm};\ l_p = 126.6 \text{ mm};\ f_{r\infty} = 5.27 \text{ MPa};\ r = 0.5 \quad (29)$$

Table 2 shows the fitted values of these parameters in different start point or different values of bounds. It is apparent that the method is dependent on the selection of bounds and start points. For instance, in Try 1, the bounds were selected $(-\infty,+\infty)$ and the start points were arbitrary, this conditions lead to a convergence problem. In Try 2 to Try 5, the start points were selected in order to be close to that reported in Eq. (29). However, the bounds were different. It can be seen through Table 2 that the fitted equations were completely different and none of them was similar to the reported values in Eq. (29). Hence, nonlinear regression could lead to different answers and should be avoided if possible. These explanations also hold in Levenberg-Marquardt method. In addition, the use of latter method should be avoided in non-convex problems.

The other point was the ambiguity in the use of shape factor, which was discussed in section 2.

5.2 The results of the proposed method

As stated previously, for determination of fracture parameters, the values of nominal stress, a_1^*, a_3^*, and a_5^*, should be determined. Then, by using linear regression analysis for each series (i.e., α=0.3, α=0.15, α=0.075, α=0.025, or α=0), the asymptotic values of fracture energy, fracture toughness, and effective length of fracture process zone should be obtained. Fig. 2 shows an illustration of the linear regression analysis of group AL0.3. It can be seen that the slope and intercept of the fitted line were p=22.618, and q=147.71 m^{-1}, respectively. Therefore, the values of fracture toughness (K_{IC}) and the size independent length of FPZ, could be determined as $K_{IC} = f_t\sqrt{-4\pi\frac{g(\alpha_0)}{g'(\alpha_0)}B_0} = 43.828$ MPa.mm$^{0.5}$, and 5.45 mm, respectively. Moreover, based on the well-known relation between fracture toughness and energy ($K_{IC} = \sqrt{EG_f}$), the value of fracture energy is equal to 46.46 N/m. The determined values of p, q, a_1^*, a_3^*, a_5^*, K_{IC}, and G_f are reflected in Table 3. It should be noted that when a/d=0, Eq. (18) is not solvable. To remedy this situation, the concept of exact solution for three point bending, which can be found in theory of elasticity books such as Timoshenko and Goodier (1951), is used. They stated that the normal stress does not follow a linear law and the exact stress in the tensile face of the beam is smaller than that is expected from the elementary beam theory (Timoshenko and Goodier 1951). Assuming that this variation is due to stress redistribution in the tensile face, one can find the effective depth of stress redistribution layer for S/d=2.176 by comparing the exact and elementary values of bending stress in tensile face as

$$\psi = \frac{\sigma_{Exact}}{\sigma_{Elementary}} = 0.844 \rightarrow \frac{d_{Exact}}{d_{Elementary}} = 0.9187 \rightarrow \rightarrow \alpha_{eq} = 0.0815 \quad (30)$$

By using this simplifying assumption, the fracture parameters for specimens with no notch are determined. Are they real? Not really. These values are not true and should be avoided in determination of fracture parameters. However, they could be used for predicting the load carrying capacity of the specimens with no notch. This

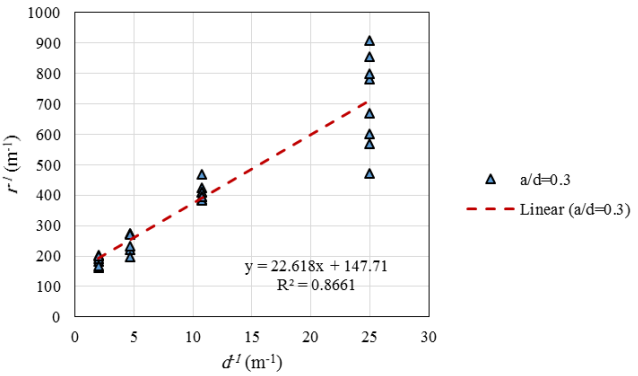

Fig. 2 The linear curve fitting for series AL0.3

Table 3 Fracture parameters for different a/d ratios

	AL0.3	AL0.15	AL0.075	AL0.025	AL0.0
p	22.618	20.363	17.963	75.368	15.226
q (m^{-1})	147.71	148.69	170.28	140.16	37.755
a_1^*	0.3806	0.2527	0.1840	0.1113	0.1910
a_3^*	-0.2641	-0.0471	0.1480	0.4067	0.1241
a_5^*	-0.1766	-0.1594	0.058	0.9364	0.0064
G_f (N/m)	46.46	46.01	40.48	49.62	168.84
K_{IC} (MPa.mm$^{0.5}$)	43.83	43.68	40.82	44.99	86.69
r_∞ (mm)	6.8	6.8	5.9	7.13	26.5

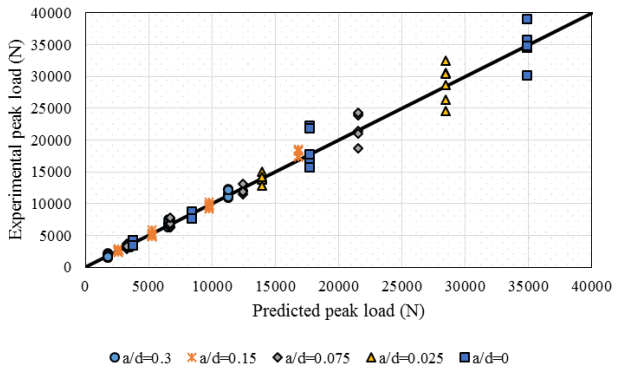

Fig. 3 Predicted peak loads versus experimental peak loads

Table 4 Coefficients of variation of predictions for different series

	AL0.3	AL0.15	AL0.075	AL0.025	AL0.0
C.O.V (%)	5.951	6.152	8.764	8.604	9.369

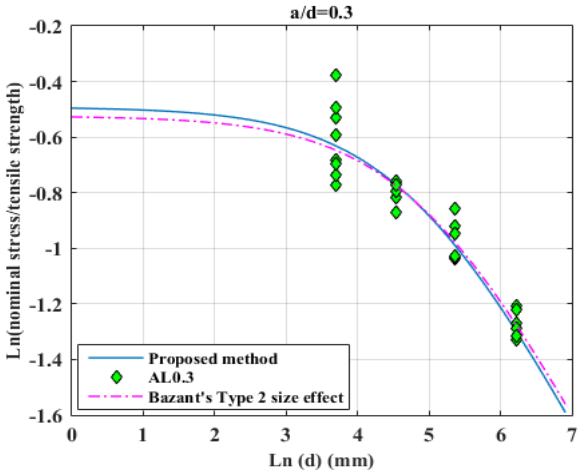

Fig. 4 Size effect plot for *a/d*=0.3

disability is similar to Bazant's method (Hoover and Bažant 2014). Hoover and Bazant stated that the Type 1 size effect should not be used in determination of fracture parameters.

Fig. 3 shows the values of predicted peak loads versus experimental peak loads. As can be seen, the proposed model could predict the values of peak loads with good precisions. To compare the workability of the model in different *a/d* ratios, the coefficients of variation for all series were determined and tabulated in Table 4. It is apparent that the reliability of the model decreases as the *a/d* ratio decreases. However, the amounts of errors are still negligible.

Fig. 4 shows the size effect plot for AL0.03 based on Eq. (26). It is clear that as the depth of specimen increases, the behavior of the specimen approaches LEFM. Besides, the method is in close agreement with Bazant's size effect law in this series. It should be noted that proposing this method does not infer weakness of Bazant's approach in prediction of load carrying capacity of specimens. However, the proposed method could make inclusion of T-stress effects and 3-d effects in the size effect study possible, since it uses Williams's expansion and higher order terms.

Table 5 Reported values for fracture energy and effective length of fracture process zone by different methods

Type 2		Type 2		USSEL	
α=0.3		α=0.15		α=0.3, α=0.15	
G_f (N/m)	C_f (mm)	G_f (N/m)	C_f (mm)	G_f (N/m)	C_f (mm)
51.9	28	49.8	21.0	56.25	29.79

Although these effects did not studied in the present paper, some researchers such as Lazzarin, Berto, Kotousov, Ayatollahi, Akbardoost and Pook conducted many experimental and theoretical researches in the mentioned field (Ayatollahi and Akbardoost 2013, Akbardoost and Rastin 2015, He *et al*. 2016, Berto *et al*. 2017, Cendón *et al*. 2017, Heydari-Meybodi *et al*. 2017, Pook *et al*. 2017).

In order to compare the results of the method with those methods, which were extensively developed by Bazant and his co-workers, the results of the USSEL, Type 2, and Type 1 size effect are reflected in this section. Table 5 shows the values reported for the series, using Type 1 and Type 2 (Hoover and Bažant 2013), and USSEL (Hoover and Bažant 2014). It is clear that the values of fracture energy in the methods are in close agreement with each other, whereas the asymptotic values for effective length of fracture process zone is different. These differences could be attributed to different assumptions, which were extensively explained in Eqs. (20) and (21).

Fig. 5 shows the size effect plots for different *a/d* ratios. It is apparent that the proposed method can capture the effects of specimens' sizes in different a/d ratios. In addition, it is clear that the parameters, reflected in Eq. (29), did not match with the experiments. This could be attributed to the typographical errors in (Hoover and Bažant 2013, Hoover and Bažant 2014), or wrong convergence of the trust-region-reflective method. Moreover, the Type 2 size effect law of Bazant was depicted for series AL0.3 and AL0.15. As was expected, the two of the methods are in close agreement. Based on Hoover and Bazant's study (Hoover and Bažant 2014), the Type 2 size effect could not predict the behavior of specimens with relatively shallow notches. On the other hand, the proposed method is shown to be able to predict the behavior of structure with shallow to deep notches.

6. Conclusions

In the present study, an efficient algorithm has been proposed in which neither separate size effect laws nor comprehensive nonlinear regression is needed. Besides, by using the exact beam theory, concept of equivalent notch length has been introduced to handle the problems with no notches without using different size effect law. Actually, since the proposed algorithm calculates the size of fracture process zone based on fracture mechanics, it is able to handle the variation relative notch length as well as the effect of boundaries. Moreover, it was shown that the method could predict the failure loads of the beams with good precisions. From the obtained results of this investigation, the following conclusions could be drawn:

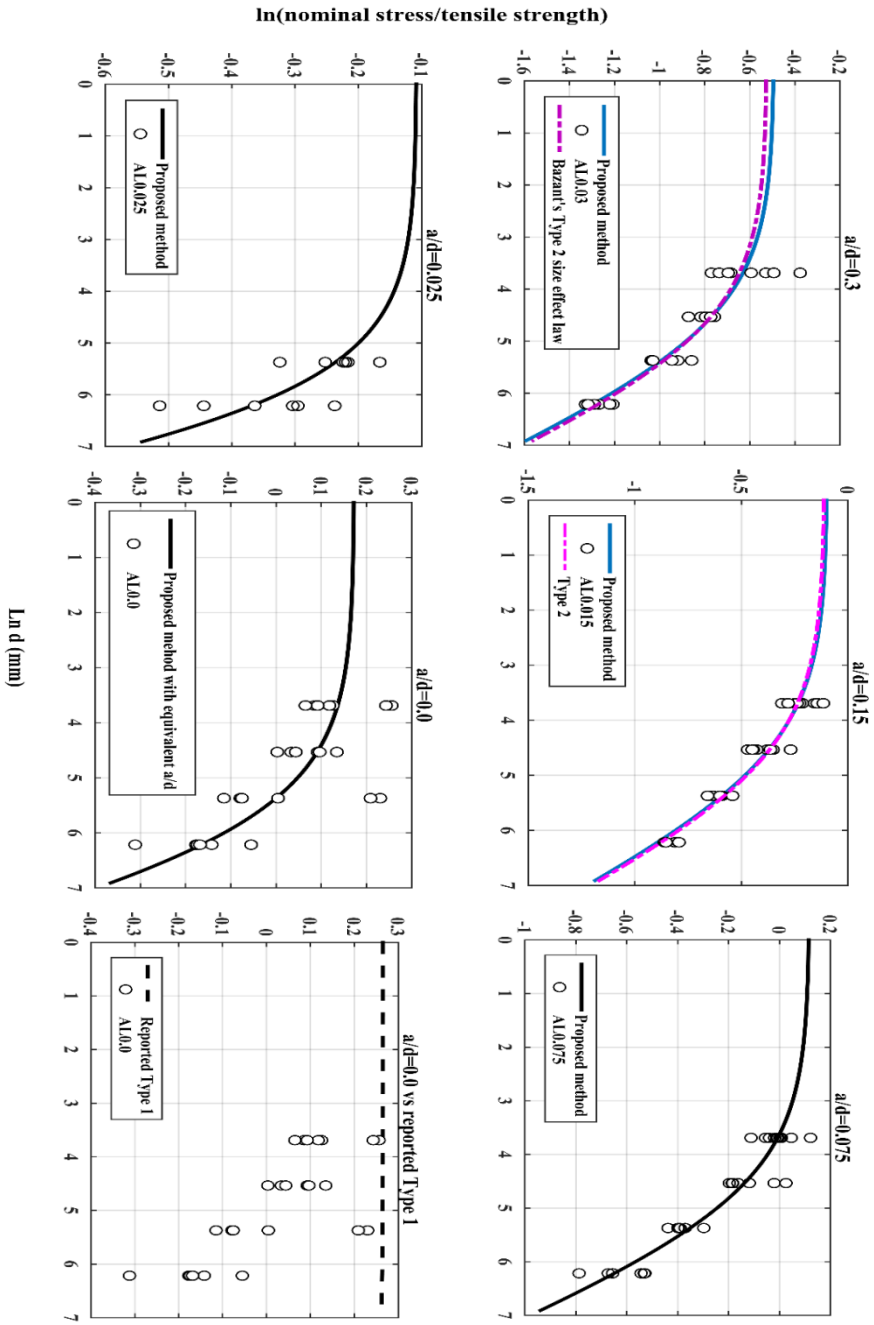

Fig. 5 Size effect plots of the proposed method

1- The proposed method is able to predict the failure loads of specimens with shallow to deep notches with good precisions.

2- By using the equivalent crack length for specimen with no notches, the method is able to predict the size effects.

3- The method is able to reflect the effects of higher order terms of stress fields on fracture parameters of concrete.

4- In the presented algorithm, the size of fracture process zone should be calculated by means of Williams's expansion. To do so, it was assumed that the onset of the crack occurs when the normal-to-crack component of stress reaches tensile strength. This procedure makes the method able to track the influence of the size of fracture process zone on size effect phenomenon.

The derivation of the size of fracture process zone was based on experiment and the assumption that the onset of crack is when the normal-to-crack component of stress reaches tensile strength. Therefore, the values of fracture process zone effective length could be somehow more reliable than the method in which this length is obtained indirectly from other fracture parameters.

5- The difficulty, raised due to the use of nonlinear regression analysis, could be circumvented by using the proposed method.

Acknowledgments

The authors wish to acknowledge all supports of Shahid Rajaee Teacher Training University.

References

Aissaoui, N. and Matallah, M. (2017), "A mesoscale investigation on the size effect of the fracture characteristics in concrete", *Int. J. GEOMATE*, **12**(32), 126-133.

Akbardoost, J. and Rastin, A. (2015), "Comprehensive data for calculating the higher order terms of crack tip stress field in disk-type specimens under mixed mode loading", *Theor. Appl. Fract. Mech.*, **76**, 75-90.

Alyhya, W.S., Abo Dhaheer, M.S., Al-Rubaye, M.M. and Karihaloo, B.L. (2016), "Influence of mix composition and strength on the fracture properties of self-compacting concrete", *Constr. Build. Mater*, **110**, 312-322.

Ayatollahi, M.R. and Akbardoost, J. (2012), "Size effects on fracture toughness of quasi-brittle materials-A new approach", *Eng. Fract. Mech.*, **92**, 89-100.

Ayatollahi, M.R. and Akbardoost, J. (2013), "Size and geometry effects on rock fracture toughness: Mode I fracture", *Rock Mech. Rock Eng.*, **47**(2), 677-687.

Ayatollahi, M.R. and Akbardoost, J. (2013), "Size effects in mode II brittle fracture of rocks", *Eng. Fract. Mech.*, **112-113**, 165-180.

Ayatollahi, M.R. and Nejati, M. (2011), "Determination of NSIFs and coefficients of higher order terms for sharp notches using finite element method", *Int. J. Mech. Sci.*, **53**(3), 164-177.

Bazant, Z. and Pfeiffer, P. (1987), "Determination of fracture energy from size effect and brittleness number", *ACI Mater. J.*, **84**(6), 463-480.

Bazant, Z.P. (1984), "Size effect in blunt fracture: concrete, rock, metal", *J. Eng. Mech.*, **110**(4), 518-535.

Bazant, Z.P. and Becq-Giraudon, E. (2002), "Statistical prediction of fracture parameters of concrete and implications for choice of testing standard", *Cement Concrete Res.*, **32**, 529-556.

Bazant, Z.P., Gettu, R. and Kazemi, M.T. (1991), "Identification of nonlinear fracture properties from size effect tests and structural analysis based on geometry-dependent r -curves", *Int. J. Rock Mech. Min. Sci.*, **28**, 43-51.

Bazant, Z.P. and Kazemi, M.T. (1990), "Determination of fracture energy, process zone length and brittleness number from size effect, with application to rock and concrete", *Int. J. Fract.*, **44**, 111-131.

Bazant, Z.P., Kim, J.K. and Pfeiffer, P.A. (1986), "Nonlinear fracture properties from size effect tests", *J. Struct. Eng.*, **112**.

Bazant, Z.P. and Oh, B.H. (1983), "Crack band theory for fracture of concrete", *Mater. Struct.*, **16**, 155-177.

Bazant, Z.P. and Planas, J. (1998), *Fracture and Size Effect in Concrete and Other Quasi-Brittle Materials*, CRC Press

Bazant, Z.P. and Yu, Q. (2009), "Universal size effect law and effect of crack depth on quasi-brittle structure strength", *J. Eng. Mech.*, **135**(2), 78-84.

Berto, F., Ayatollahi, M.R., Vantadori, S. and Carpinteri, A. (2017), "Review of the Influence of non-singular higher order terms on the stress field of thin welded lap joints and small inclined cracks in plates", *Frattura ed Integrità Strutturale*, **41**, 260-268.

Berto, F., Kotousov, A., Lazzarin, P. and Pegorin, F. (2013), "On a coupled mode at sharp notches subjected to anti-plane loading", *Eur. J. Mech., A/Solid.*, **38**, 70-78.

Berto, F. and Lazzarin, P. (2010), "On higher order terms in the crack tip stress field", *Int. J. Fract.*, **161**(2), 221-226.

Berto, F. and Lazzarin, P. (2013), "Multiparametric full-field representations of the in-plane stress fields ahead of cracked components under mixed mode loading", *Int. J. Fatig.*, **46**, 16-26.

Berto, F., Lazzarin, P. and Ayatollahi, M.R. (2013), "Recent Developments in Brittle and Quasi-Brittle Failure Assessment of Graphite by Means of SED", *Key Eng. Mater.*, **577-578**, 25-28.

Berto, F., Lazzarin, P. and Kotousov, A. (2011), "On higher order terms and out-of-plane singular mode", *Mech. Mater.*, **43**(6), 332-341.

Cedolin, L. and Cusatis, G. (2008), "Identification of concrete fracture parameters through size effect experiments", *Cement Concrete Compos.*, **30**(9), 788-797.

Cendón, D.A., Jin, N., Liu, Y., Berto, F. and Elices, M. (2017), "Numerical assessment of gray cast iron notched specimens by using a triaxiality-dependent cohesive zone model", *Theor. Appl. Fract. Mech.*, **90**, 259-267.

Cifuentes, H. and Karihaloo, B.L. (2013), "Determination of size-independent specific fracture energy of normal- and high-strength self-compacting concrete from wedge splitting tests", *Constr. Build. Mater*, **48**, 548-553.

Coleman, T.F. and Li, Y. (1992), "On the convergence of interior-reflective Newton methods for nonlinear minimization subject to bounds", *Math. Program.*, **67**(1), 189-224.

Coleman, T.F. and Li, Y. (1996), "An interior trust region approach for nonlinear minimization subject to bounds", *SIAM J. Optim.*, **6**(2), 418-445.

Cusatis, G. and Schauffert, E.A. (2009), "Cohesive crack analysis of size effect", *Eng. Fract. Mech.*, **76**(14), 2163-2173.

Duan, K. and Hu, X. (2004), *Scaling of Specimen Boundary Effect on Quasi-Brittle Fracture*, Brisbane, Australia.

Duan, K., Hu, X. and Wittmann, F.H. (2003), "Boundary effect on concrete fracture and non-constant fracture energy distribution", *Eng. Fract. Mech.*, **70**(16), 2257-2268.

Duan, K., Hu, X. and Wittmann, F.H. (2006), "Scaling of quasi-brittle fracture: Boundary and size effect", *Mech. Mater.*, **38**(1-2), 128-141.

Duan, K., Hu, X. and Wittmann, F.H. (2007), "Size effect on specific fracture energy of concrete", *Eng. Fract. Mech.*, **74**(1-2), 87-96.

He, Z., Kotousov, A., Berto, F. and Branco, R. (2016), "A brief review of recent three-dimensional studies of brittle fracture", *Phys. Mesomech.*, **19**(1), 6-20.

Heydari-Meybodi, M., Ayatollahi, M.R., Dehghany, M. and Berto, F. (2017), "Mixed-mode (I/II) failure assessment of rubber materials using the effective stretch criterion", *Theor. Appl. Fract. Mech.*, **91**, 126-133.

Hillerborg, A., Modeer, M. and Petersson, P.E. (1976), "Analysis of crack formation and crack growth in concrete by means of fracture mechanics and finite elements", *Cement Concrete Res.*, **6**, 773-782.

Hoover, C.G. and Bažant, Z.P. (2014), "Cohesive crack, size effect, crack band and work-of-fracture models compared to comprehensive concrete fracture tests", *Int. J. Fract.*, **187**(1), 133-143.

Hoover, C.G. and Bažant, Z.P. (2014), "Comparison of the hu-duan boundary effect model with the size-shape effect law for quasi-brittle fracture based on new comprehensive fracture tests", *J. Eng. Mech.*, **140**(3), 480-486.

Hoover, C.G. and Bažant, Z.P. (2014), "Universal size-shape effect law based on comprehensive concrete fracture tests", *J. Eng. Mech.*, **140**(3), 473-479.

Hoover, C.G. and P. Bažant, Z. (2013), "Comprehensive concrete fracture tests: Size effects of Types 1 & 2, crack length effect and postpeak", *Eng. Fract. Mech.*, **110**, 281-289.

Hoover, C G., Bažant, Z.P., Vorel, J., Wendner, R. and Hubler, M.H. (2013), "Comprehensive concrete fracture tests:

Description and results", *Eng. Fract. Mech.*, **114**, 92-103.
Hu, X. and Duan, K. (2004), "Influence of fracture process zone height on fracture energy of concrete", *Cement Concrete Res.*, **34**(8), 1321-1330.
Hu, X. and Duan, K. (2007), "Size effect: Influence of proximity of fracture process zone to specimen boundary", *Eng. Fract. Mech.*, **74**(7), 1093-1100.
Hu, X. and Duan, K. (2009), "Size effect and quasi-brittle fracture: the role of FPZ", *Int. J. Fract.*, **154**(1-2), 3-14.
Hu, X., Guan, J., Wang, Y., Keating, A. and Yang, S. (2017), "Comparison of boundary and size effect models based on new developments", *Eng. Fract. Mech.*, **175**, 146-167.
Duan, K., Hu, X.Z. and Wittmann, F.H. (2003), "Size effect on fracture resistance and fracture energy of concrete", *Mater. Struct.*, **36**(2), 74-80.
Karamloo, M., Mazloom, M. and Payganeh, G. (2016), "Effects of maximum aggregate size on fracture behaviors of self-compacting lightweight concrete.", *Constr. Build. Mater.*, **123**, 508-515.
Karamloo, M., Mazloom, M. and Payganeh, G. (2016), "Influences of water to cement ratio on brittleness and fracture parameters of self-compacting lightweight concrete", *Eng. Fract. Mech.*, **168 Part A**, 227-241.
Karamloo, M., Mazloom, M. and Payganeh, G. (2017), "Effect of size on nominal strength of self-compacting lightweight concrete and self-compacting normal weight concrete: A stress-based approach", *Mater. Today Commun.*, **13**, 36-45.
Karihaloo, B.L. (1999), "Size effect in shallow and deep notched quasi-brittle structures", *Int. J. Fract.*, **95**, 379-390.
Karihaloo, B.L., Abdalla, H.M. and Xiao, Q.Z. (2003), "Size effect in concrete beams", *Eng. Fract. Mech.*, **70**(7-8), 979-993.
Karihaloo, B.L., Murthy, A.R. and Iyer, N.R. (2013), "Determination of size-independent specific fracture energy of concrete mixes by the tri-linear model", *Cement Concrete Res.*, **49**, 82-88.
Karihaloo, B.L. and Xiao, Q.Z. (2001), "Accurate determination of the coefficients of elastic crack tip asymptotic field by a hybrid crack element with p-adaptivity", *Eng. Fract. Mech.*, **68**(15), 1609-1630.
Karihaloo, B.L. and Xiao, Q.Z. (2001), "Higher order terms of the crack tip asymptotic field for a notched three-point bend beam", *Int. J. Fract.*, **112**, 111-128.
Karihaloo, B.L. and Xiao, Q.Z. (2001), "Higher order terms of the crack tip asymptotic field for a wedge-splitting specimen", *Int. J. Fract.*, **112**, 129-137.
Karihaloo, B.L. and Xiao, Q.Z. (2007), *Accurate Simulation of Frictionless and Frictional Cohesive Crack Growth in Quasi-Brittle Materials Using XFEM*, Springer Netherlands, Dordrecht.
Karihaloo, B.L. and Xiao, Q.Z. (2008), "Asymptotic fields at the tip of a cohesive crack", *Int. J. Fract.*, **150**(1-2), 55-74.
Karihaloo, B.L. and Xiao, Q.Z. (2010), "Asymptotic fields ahead of mixed mode frictional cohesive cracks", *ZAMM - J. Appl. Math. Mech., Zeitschrift für Angewandte Mathematik und Mechanik*, **90**(9), 710-720.
Khoramishad, H., Akbardoost, J. and Ayatollahi, M. (2013), "Size effects on parameters of cohesive zone model in mode I fracture of limestone", *Int. J. Damage Mech.*, **23**(4), 588-605.
Kotousov, A., Lazzarin, P., Berto, F. and Harding, S. (2010), "Effect of the thickness on elastic deformation and quasi-brittle fracture of plate components", *Eng. Fract. Mech.*, **77**(11), 1665-1681.
Lei, W.S. (2018), "A generalized weakest-link model for size effect on strength of quasi-brittle materials", *J. Mater. Sci.*, **53**(2), 1227-1245.
Leicester, R. (1969). "The size effect of notches.", *Proceedings of the Second Australasian Conference on Mechanics of Materials and Structures.*, Melbourne.
Li, M., Hao, H., Shi, Y. and Hao, Y. (2018), "Specimen shape and size effects on the concrete compressive strength under static and dynamic tests", *Constr. Build. Mater*, **161**, 84-93.
Li, Z. and Pasternak, H. (2018), "Statistical size effect of flexural members in steel structures", *J. Constr. Steel Res.*, **144**, 176-185.
Liu, H.Z., Lin, J.S., He, J.D. and Xie, H.Q. (2018), "Discrete elements and size effects", *Eng. Fract. Mech.*, **189**, 246-272.
Malíková, L. and Veselý, V. (2015), "The influence of higher order terms of Williams series on a more accurate description of stress fields around the crack tip", *Fatig. Fract. Eng. Mater. Struct.*, **38**(1), 91-103.
Mazloom, M., Allahabadi, A. and Karamloo, M. (2017), "Effect of silica fume and polyepoxide-based polymer on electrical resistivity, mechanical properties, and ultrasonic response of SCLC", *Adv. Concrete Constr.*, **5**(6), 587-611.
Moré, J.J. (1978), *The Levenberg-Marquardt algorithm: Implementation and theory*, Springer Berlin Heidelberg
Muralidhara, S., Raghu Prasad, B.K., Karihaloo, B.L. and Singh, R.K. (2011), "Size-independent fracture energy in plain concrete beams using tri-linear model", *Constr. Build. Mater*, **25**(7), 3051-3058.
Needleman, A. (2018), "Effect of size on necking of dynamically loaded notched bars", *Mech. Mater.*, **116**, 180-188.
Owen, D.R.J. and Fawkes, A.J. (1983), *Engineering Fracture Mechanics: Numerical Methods and Applications*, Pineridge Press Ltd., Swansea, UK.
Pook, L.P. (2013), "A 50-year retrospective review of three-dimensional effects at cracks and sharp notches", *Fatig. Fract. Eng. Mater. Struct.*, **36**(8), 699-723.
Pook, L.P., Berto, F. and Campagnolo, A. (2017), "State of the art of corner point singularities under in-plane and out-of-plane loading", *Eng. Fract. Mech.*, **174**, 2-9.
Yu, Q., Le, J.L., Hoover, C.G. and Bažant, Z.P. (2010), "Problems with Hu-Duan boundary effect model and its comparison to size-shape effect law for quasi-brittle fracture", *J. Eng. Mech.*, **136**(1), 40-50.
Ramachandra Murthy, A., Karihaloo, B.L., Iyer, N.R. and Raghu Prasad, B.K. (2013), "Bilinear tension softening diagrams of concrete mixes corresponding to their size-independent specific fracture energy", *Constr. Build. Mater*, **47**, 1160-1166.
Ramachandra Murthy, A., Karihaloo, B.L., Iyer, N.R. and Raghu Prasad, B.K. (2013), "Determination of size-independent specific fracture energy of concrete mixes by two methods", *Cement Concrete Res.*, **50**, 19-25.
Rong, G., Peng, J., Yao, M., Jiang, Q. and Wong, L.N.Y. (2018), "Effects of specimen size and thermal-damage on physical and mechanical behavior of a fine-grained marble", *Eng. Geology*, **232**, 46-55.
Timoshenko, S.P. and Goodier, J.N. (1951), *Theory of Elasticity*, McGraw Hill, New York.
Tong, P., Pian, T.H.H. and Lasry, S.J. (1973), "A hybrid-element approach to crack problems in plane elasticity", *IJNME*, **7**(3), 297-308.
Wan-Wendner, L., Wan-Wendner, R. and Cusatis, G. (2018), "Age-dependent size effect and fracture characteristics of ultra-high performance concrete", *Cement Concrete Compos.*, **85**, 67-82.
Weibull, W. (1939). *A Statistical Theory of the Strength of Materials*, Stockholm.
Weibull, W. (1951), "A statistical distribution function of wide applicability.", *J. Appl. Mech*, **18**(3), 293-297.
Williams, M.L. (1961), *The Bending Stress Distribution at the Base of a Stationary Crack*, ATJEM.
Xiao, Q. and Karihaloo, B.L. (2006), "Asymptotic fields at frictionless and frictional cohesive crack tips in quasibrittle materials", *J. Mech. Mater. Struct.*, **1**(5), 881-910.

Xiao, Q.Z. and Karihaloo, B.L. (2007), "An overview of a hybrid crack element and determination of its complete displacement field", *Eng. Fract. Mech.*, **74**(7), 1107-1117.
Yoo, D.Y. and Yang, J.M. (2018), "Effects of stirrup, steel fiber, and beam size on shear behavior of high-strength concrete beams", *Cement Concrete Compos.*, **87**, 137-148.
Zappalorto, M. and Lazzarin, P. (2013), "Three-dimensional elastic stress fields ahead of notches in thick plates under various loading conditions", *Eng. Fract. Mech.*, **108**, 75-88.

CC

Nomenclature

a	Crack length
a_0	Notch length
a_n	Coefficients of Williams's expansion
A_0	Empirical coefficient
b	Beam width
B_0	Empirical coefficient
c_f	Effective length of fracture process zone in Bazant's method
d	Beam depth
$\bar{D}$	Depth of beam with no notch in Bazant's method
D_b	Empirical coefficient
E	Modulus of elasticity
f_t	Tensile strength
$f_{r\infty}$	Empirical coefficient
$g_f(\alpha)$	Non-dimensional energy release rate function
G_f	Initial fracture energy
k	Empirical coefficient
K_C	Apparent toughness
K_{IC}	Fracture toughness
l_p	Empirical coefficient
L	Length of the beam
r	Size dependent length of fracture process zone
r_∞	Size independent length of fracture process zone
S	Span of the beam
σ_N	Nominal stress
ε	Strain
$\varepsilon_{,n}$	Strain gradient
ψ	Shape factor
FPZ	Fracture process zone
USSEL	Universal size-shape effect law